Monitoring color alteration of ornamental flagstones using digital image analysis.

V. Lebrun, C. Toussaint & E.Pirard
Université de Liège, GeomaC, Géoressources Minérales, Liège, Belgium.

ABSTRACT: This paper presents a methodology for quantifying color alteration of dimensions stones as caused by weathering using digital image analysis. Specific imaging methods are suggested for color calibration and geometric repositioning and practical solutions are provided in order to account for spatio-temporal drift and optical aberration. The procedure consists in grabbing and comparing images of polished granite flagstones before and after accelerated ageing tests. This method is non-destructive, allowing pre-weathering and post-weathering image acquisition on the same sample after repositioning with an accuracy of 0.4 millimeters. Color alteration is computed using a Euclidean distance in a (pseudo)-L*a*b* color space. The results of a practical study on three selected granites are presented and discussed.

1 INTRODUCTION

The aim of this paper is to propose technical solutions and analytic methods for monitoring the color decay caused by weathering using digital image analysis. The mineralogy of three selected granites is first briefly described, followed by an overview of the complete testing protocol. The two main sections develop the calibration procedure for the imaging system and the image analysis methodology. Finally, the most significant results are presented and commented. A brief discussion about potential extensions of the proposed techniques and its limitations conclude the subject.

The quantitative description of the behavior of ornamental stones submitted to natural or artificial weathering is a crucial challenge not only scientific but also economic. This is indeed one of the most important characteristics of these materials, determining their field of use in the building market. Mineralogical or geochemical mechanisms of rock alteration have been widely studied (Delvigne 1998). Some works have been performed trying to quantify the degradation of mechanical and physical properties (De Cleene 1995), but very little information is available about the aesthetic alteration of stones after weathering. However, from the consumer's point of view, this aesthetic point of view is probably the most important one. For example, any deviation, even slight, in the predominant color of adjacent tiles in a paving badly affects the aesthetic of the work as a whole by emphasizing the color discontinuity induced by the cement joints.

Of course, standard colorimeters or spectrophotometers are available for quantitative measurements of color. But both devices integrate very limited fields of investigation (typically = 1cm²). They are thus largely irrelevant for monitoring color variations in textured materials like granites.

The idea of using digital image analysis to characterize or control the quality of ornamental stones (Muge et al. 1997) or ceramics (Baldrich et al. 1999) is not a revolutionary idea. For the last five years various consortiums have been managing ambitious research programs at European level with the aim of integrating automatic inspection systems for ceramic tiles (Maccari 1998, Donia 2000). This recent interest for quantitative color quality control by digital video camera confirms the potentiality of the technique and reflects the need for an accurate and objective tool to control the visual aspect of tiles in the stone industry.

The present work tries to go one step further by integrating color image analysis into a wider timescale, which leads to the notions of color alteration and color durability. The testing methods presented here are first available in laboratory but could be extended, with some limitations, to "in situ" paving on facades and to natural outcrops of stones.

2 MATERIALS AND METHODS

2.1 Selection of granites

For this study, three granites have been selected especially according to their high propensity to chromatic alteration (Elsen 1996). Table 1 presents the names, nature, origin and mineralogy of the granites.

Table 1. Name, origin and mineralogy of the selected granites. Albite (Ab), Microcline (Mc), Quartz (Qz), Biotite (Bt), Hornblende (Hb), Kaolinite (Kl), Chlorite (Cl).

Name	Nature	Origin	Mineralogy		
			Princ.	*Second.*	*Access.*
Tarn	Granite	France	Ab Mc Qz Bt		Kl Cl
Azul Paveno	Gneiss	Brazil	Ab Mc Qz	Bt	Kl
Baltic Brown	Wiborgite (granite)	Finland	Ab Mc Qz	Bt Hb	

Three polished flags (300 mm x 300 mm) of each granite have been sampled and submitted to the analysis procedure. The tiles have been randomly selected among a daily production of the quarries.

2.2 General testing protocol.

For future normative tasks one has defined a rigorous protocol of test having a care for generality and reliability. Each fresh sample is first imaged and its initial color statistics are computed and stored. The tiles are then submitted to defined accelerated ageing tests. After precise repositioning under the imaging system, a second color image is acquired from which final color statistics are extracted. The color alteration is computed from a pixel to pixel comparison of the pre-weathering and post-weathering images.

2.3 Accelerated ageing tests

The ageing chamber used is a KSE-300 designed for the realization of corrosion tests following the DIN50017 and DIN 50018 norms (DIN 1982, 1997) and for alternating condensation controls.
The following normalized tests have been performed:

1. Acid test (two samples of each granite): 21 days at 20°C in a SO2 saturated atmosphere.
2. Water and heat test (one sample of each granite): 21 heating cycles during 20 hours in a ventilated drying-room at 105°C followed by 4 hours in a water bath at 20°C.

These tests have been chosen for two main reasons: First, Elsen (1996) observed some visually significant color changes in the same granites submitted to the acid test. Second, both tests are using oxidant atmospheres suitable for modeling the urban environment to which external wall covering tiles could be submitted during their life.

2.4 Imaging devices.

A specific acquisition system has been designed taking into account the optical properties of the observed samples. The three main characteristics of polished granite tiles are:

- macroscopic dimensions (300 mm by 300 mm),
- high reflectivity
- textured color

These properties induce technical constraints on the imaging system (Lebrun et al. 1999) which needs to capture diffuse reflectance from a daylight source while maintaining a stable response in time. In practice, the final solution adopted for this study is an imaging chamber equipped with high frequency “daylight” fluorescent tubes, diffusing walls and a high resolution black and white CCD sensor fitted with a filter wheel bearing red, green and blue gelatin filters.

3 IMAGE CALIBRATION AND ANALYSIS.

Like for any other scientific instrument, each step of the image acquisition with a CCD-camera has to be controlled and calibrated. The lighting system, the optics and the electronic devices all induce noise and color deviations that must be checked for stability and uniformity of response through time and space.

3.1 Corrections for temporal noise and drift.

A low frequency drift of the video signal with time is due to a progressive heating up of the CCD sensor. In order to minimize this, it is recommended to switch on the camera for about one to two hours before operating (Pirard et al. 1999).

A high frequency component in the signal variation with time is due to both electronic and thermal noise (Holst 1998). Such noise can reasonably be filtered by time-averaging a sequence of sixteen images.

3.2 Corrections for spatial noise and drift

Even with an almost ideal acquisition system, non-uniform illumination and optical aberrations will induce a low frequency drift across the field of view.
This can be corrected for by taking two reference images : - the first one is a “black noise” image obtained by grabbing a picture from the camera when preventing any light to hit the sensor; - the second one is a “white reference” image obtained by picturing a surface sprayed with barium sulfate or alternatively a plate of glossy white high density polyethyl-

ene (PEHD) under exactly the same imaging conditions as those used for the whole study.

From both the black and white reference images it is possible to achieve a numerical gain and offset adjustment of each individual pixel so as to obtain a perfectly homogeneous response from a mineral no matter where it lies in the scene (Pirard et al. 1999).

3.3 Color calibration

Each optical component of the acquisition device induces deviation of the output red green and blue channel compared to the intrinsic color of the observed material. These errors can be numerically corrected by calibrating the system with standardized color charts. Various solutions are available to perform this calibration (Connolly & Leung 1995; Chang & Reid 1996; Marszalec & Pietikäinen 1997). The common goal is to compute the transfer-matrix of the imaging tool, which converts the device dependant color channels (RGB) into a calibrated color system like CIE-RGB or CIE-L*a*b*.

In this study, the main objective is to quantify relative shade differences rather than absolute color values. It is thus possible to work directly with the output R, G and B value given by the camera. Nevertheless, an original procedure is used to optimize the color rendering of the system and to ensure its reliability. Each image is acquired with a standard grey scale (Kodak Q-14) present in the scene. The integration time, the gain and the offset of each channel are tuned individually in order to obtain identical mean intensities in the grey patches of the scale. Although the obtained color co-ordinates remain device dependant, this calibration ensures the reliability of the relative color deviation measure, as the same device is used for both the pre-weathering and post-weathering acquisition steps.

3.4 Positioning calibration.

In order to achieve precise repositioning of the tile under the image acquisition system after having suffered the ageing test, it is necessary to stick three targets on each tile. These spatio-referenced targets allow combining images of fresh and altered tiles with a spatial accuracy of a single pixel (0.4 mm). The image grabbing geometry is kept identical during both acquisition phases (the system being locked during the ageing tests). In this manner, the images are affected in exactly the same way by eventual lens distortion.

3.5 HSL global statistics

Global color deviations are measured on entire tiles in the hue-saturation-intensity space, HSI (Gonzalez & Woods, 1992). This is a bi-conical color space, directly deduced from RGB by linear transforms. Of course, it is non-linear and device dependant, but it presents the great advantage to be probably the most intuitive manner of specifying color. The relative pre- (IN) to post-(OUT) differences between average values of each channel are computed as follows:

$$dX = 2.\frac{\left(\overline{X}_{Out} - \overline{X}_{In}\right)}{\left(\overline{X}_{Out} + \overline{X}_{In}\right)} \tag{1}$$

where $\overline{X}_{In}$ denotes the global mean estimator of the desired channel (H, S or I) in the input image.

These values are convenient for explaining global color deviations, but they must not be considered as quantitative measures of these changes. Even a Euclidean distance in HSI space would not give such an objective quantification as it is not a linear space regarding to visual perception (Mac Adam, 1942). Nevertheless, for the industrial transfer of the methodology, the utilization of such a self-understanding color decomposition might appear necessary.

*3.6 L*a*b* local distances*

In order to map the quantitative color variation undergone by each pixel during the accelerated ageing operation, one needs to use a perceptually linear space like CIE L*a*b*. It is a uniform spherical color space especially created by the CIE for color difference computations. The transformation from R, G, B channels to L*a*b* is non-linear. For the complete description of the transfer equations, the reader is referred to the CIE recommendations (CIE, 1986).

These relationships are only relevant for calibrated CIE-RGB values. Applying the same formulas to the device dependant red, green and blue channels could make poor sense. Nevertheless, the pseudo L*a*b* has been preferred here because it will allow using the same method for CIE-L*a*b* computation in future works with a calibrated CIE-RGB input.

Once the L*a*b* co-ordinates are computed, the difference between two measured colors is given by the following relationship:

$$\Delta E_{Lab} = \sqrt{(\Delta L^*)^2 + (\Delta a^*)^2 + (\Delta b^*)^2} \tag{2}$$

In the present application, ΔL*, Δa* and Δb* are the pixel-to-pixel differences within each of the L*, a* and b* channels before and after accelerated ageing tests. This resulting distance function is then mapped into a new image in which the intensity of each pixel is proportional to the computed L*a*b* color distance.

The mean and maximum values of the distance map give a more quantitative, but less intuitive, idea of the global color deviation than the HSL statistics.

By choosing an appropriate threshold in the distance map, one can extract the most altered regions in the tiles and compute some useful statistics on them:

- Number of regions

- Relative cumulated area of all regions
- Average size of individual regions
- Mean color distance within a region

Figure 1 shows images from the sound and altered selected granites, the corresponding color distance images and the binary images resulting from the thresholding operation.

4 RESULTS

4.1 Macroscopic observations and mineralogy

The “water and heat” test did not cause any perceptive chromatic alteration. No significant color change could be visually detected. However, the parameters of this test (heat, wet, O_2 and CO_2) are expected to favor the oxidation of pyrite into limonite or goethite (Costagliola et al. 1997). The absence of this phenomenon can be due to a very low pyrite content or to a very slow kinetic of oxidation.

On the contrary, some of the samples exposed to the acid test locally underwent drastic color changes, especially those of Tarn and Baltic Brown.

Yellowish white efflorescence appeared on the three granite types. These crusts were identified by optical microscopy as composed of gypsum ($CaSO_4.2H_2O$) and are more abundant in Baltic Brown. Elsen (1998) explains this relative abundance by the presence, in the latter, of calcic hornblende, which probably acts as a catalyzer of the crystallization. He argues that this mineral contains Ca^{++} ions needed for gypsum formation and does not take a good polish, thus offering a larger specific surface for alteration.

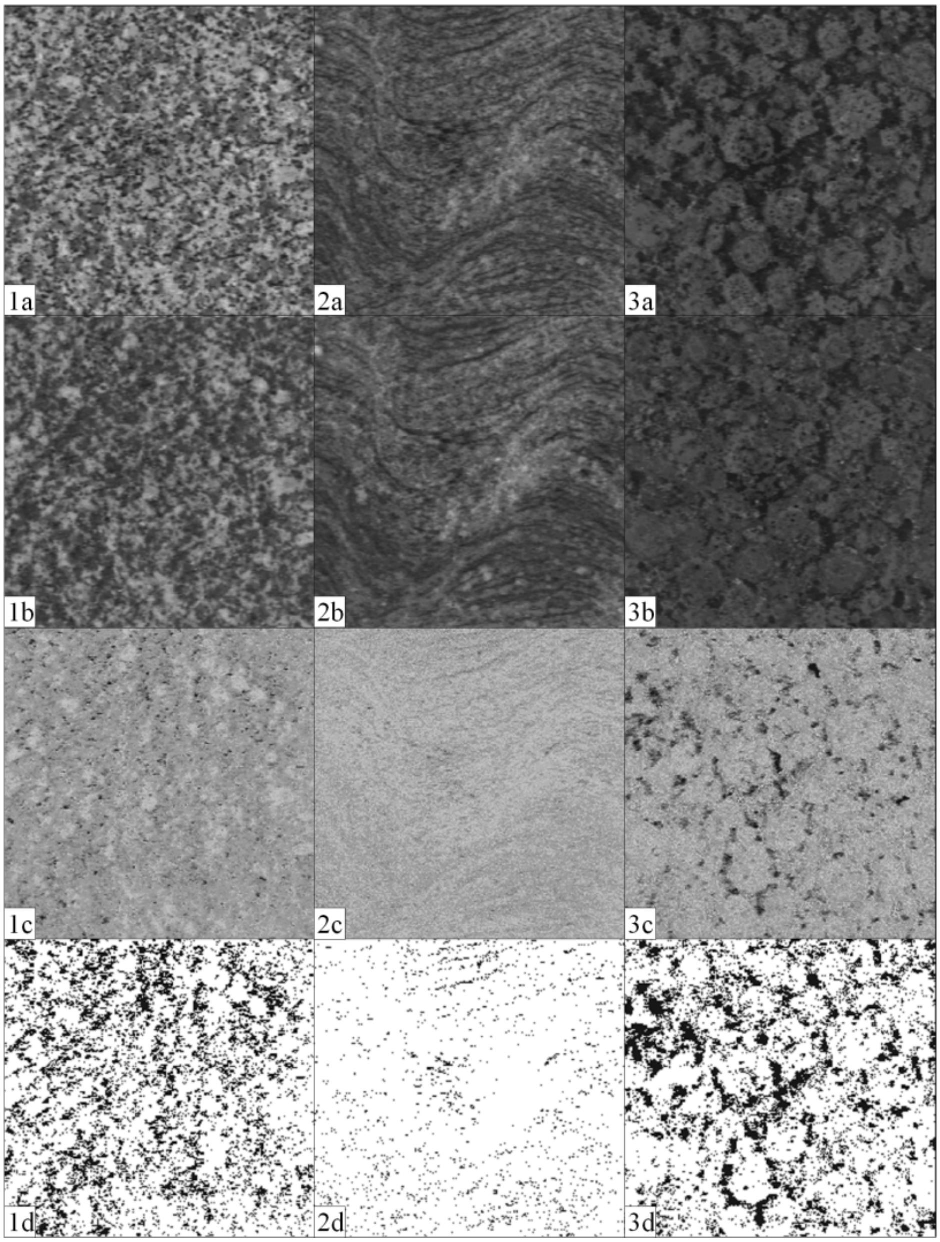

Figure 1. Selected granite tiles from Tarn (1), Azul Paveno (2) and Baltic Brown (3) imaged before (a) and after the ageing test (b). The color distance image (c) is thresholded to identify regions affected by significant changes (d)

Rust-colored patches (limonite and goethite) appear on Tarn and, to a lesser extent, on Baltic brown tiles. In both cases, a careful macroscopic observation reveals that muscovite is the preferential alteration site. Table 2 contains the relative HSI differences between fresh and altered samples computed following equation (1).

Table 2: HSI relative differences between altered and fresh samples

	ΔH (%)	ΔS (%)	ΔI (%)
Tarn	-33	+74	-28
Azul Paveno	-12	-27	+2
Baltic Brown	-26	+37	-10

Global and local statistical parameters computed from the distance images are presented in table 3. The first two columns contain the mean and maximum distances as obtained for the entire surface of the tiles. The following columns concern local information about the most altered regions obtained from thresholding the distance image at a level of 13.

Table 3: Global and local analysis of the CIE-L*a*b* colour distance images. With, A_A: cumulated surface fraction; μ(Size): average area of individual regions; μ(ΔE): mean color distance within individual regions.

	GLOBAL STATISTICS		STATISTICS ON REGIONS		
	Mean	Max	A_A (%)	μ(Size)	μ(ΔE)
Tarn	10,4	66,8	21,4	8,3	15,3
Azul Paveno	7,0	35,2	4,1	1,9	15,1
Baltic Brown	10,5	74,4	23,4	8,9	15,6

5 DISCUSSION

The HSI differences presented in table 2 are not really representative of color changes, mainly because they indicate global information when color alteration is most often localized. Nevertheless, they allow expressing visual observations into numerical terms and checking that the digital imaging system is able to model human eye perception, at least up to a certain level.

Table 3 confirms that the most important chromatic variations are observed in the Tarn and Baltic Brown granites. The intensity channel is affected by two opposite contributions: the surface state alteration tends to decrease the overall brightness, whereas the apparition of white efflorescence pushes the intensity upwards. By comparing the three granites based on ΔI, one can deduce that the tarnishing effect is predominant in Tarn and, to a lesser extent, in Baltic Brown. In Azul Paveno, both surface state and efflorescence effect compensate mutually. The sharp increase in saturation observed for Tarn and Baltic Brown is probably due to the rust colored patches having high saturation levels compared with the duller shades of natural granites.

The L*a*b* distances maps and their related parameters give a much more precise description of the intensity of color deviations. One can summarize the information from table 3 as follows:

- The mean color distances are in complete accordance with the HSI differences concerning the global alteration of each granite.
- The lower global color deviation observed in Azul Paveno is not due to a lower mean color distance in the altered sites. It results from a lower amount of altered regions combined with a smaller mean size, thus a lower surface proportion, of these regions.
- If Baltic Brown and Tarn present similar global color alterations, the spatial distribution of this alteration is somewhat different. The Tarn granite contains fewer patches, with lower mean size and lower mean distance than Baltic Brown.

6 CONCLUSIONS

From the results presented above, it can be said that digital cameras and image analysis are able to perform quantitative color measurements of large textured samples. Combined with accelerated ageing test this proves to be a powerful tool to evaluate the color deviations caused by weathering on ornamental stones.

More generally, calibrated digital image analysis appears to be a suitable tool for geologist and material science engineers in order to tackle problems of quality control of building materials, durability of stones, aesthetic alteration, etc.

6.1 Advantages and possible extensions of the method

Digital imaging is a non-destructive analytical tool. Compared to other tools used for durability assessment such as mechanical or chemical testing, measures can be achieved exactly on the same sample before and after weathering.

Questioning the adequacy and reality of the weathering tests is out of the scope of this paper. It suffices to assume that useful information about the durability and resistance of a material against weathering can be derived from such tests

In the present case, one can claim that calibrated digital image analysis is the only one method to obtain a meaningful, quantitative and reliable evaluation of the color modification.

Moreover, color is not the only physical property than can be monitored by digital imaging. Under low-angled light, pictures can be taken in which the intensity will be inversely proportional to the roughness of the surface. Using the adequate modus operandi it will be possible to quantify the loss of luster induced by weathering on polished stones.

Additionally, the exact position of altered regions can be stored in a GIS-like geographical information system together with mineralogical, chemical, micro-hardness and other data… Such a multi-data system could open a wide range of possible scientific studies on stone alteration.

Finally, the use of digital imaging devices is not restricted to laboratory experiments. Calibrated video imaging can be used to observe "in situ" the degradation of wall covering materials. Real scale studies can be set up by grabbing pictures of facades at the reception of works and comparing them with pictures taken one or two years later under the same conditions.

One step further concerns the application of image analysis to field imaging of natural outcrops (Lebrun et al. 1999). In this case, digital imaging proves to be the only way to store and retrieve quantitative information related to geometry and color of geological bodies.

6.2 Limitations

The main limitations of the imaging techniques are linked with the reliability of the image acquisition itself. If it is not possible to take pictures in exactly the same conditions (geometry, field of view, lighting), calibration will be a very delicate problem. In any case, spending time to optimize the image acquisition is never losing time. But, the information lost by using an inadequate imaging system will be lost forever.

Techniques suitable for observing flat surfaces are not readily transferable to surfaces with severe topographical gradients. Numerical shading corrections do exist, which can attenuate the problems but never eliminate them.

In a future work, it would be interesting to improve the method by computing the transfer-matrix of the system using a large reference color set (Marszalec & Pietikäinen, 1996). The color set should be chosen in order to cover the entire shade gamut of the studied granites. This would allow standardizing the measure of color alteration in the CIE-L*a*b* system.

7 REFERENCES

Baldrich, R., Vanrell, M., Villanueva, J. J. (1999) Texture-color features for tile classification. EUROPTO/SPIE Conference on Color and Polarisation Techniques in Industrial Inspection, Munich (Germany).

Chang, Y.-C. and Reid, J. (1996) RGB calibration for color image analysis in machine vision. IEEE Trans. Image Proc., 5, 10: 1414-1422.

CIE (1986) Colorimetry-Official recommendations of the International Commission on Illumination, CIE Publication N° 15.2, Vienna

Connoly, C. and Leung, T. (1995) Industrial color inspection by video camera", IEE Int. Conf. On Image Processing and its Applications, Conference publication no.410, IEE, pp. 672-676.

Costagliola, P., Cipriani, C. and Manganelli del Fa, C. (1997) Pyrite oxidation: protection using synthetic resins. European Journal of Mineralogy, 9: 167-174.

De Cleene, M. (1995) Interactive physical weathering and bioreceptivity study on building stones, monitored by computerized x-ray tomography (CT) as a potential non-destructive research tool. Commission of the European communities, directorate-general for science, research and development, Bruxelles, 286 p.

Delvigne J. (1998) Atlas of micromorphology of mineral alteration and weathering. Mineralogical association of Canada, Ottawa, 494 p.

DIN 50017-Ausgabe:1982-10 (1982) Klimate und ihre technische Anwendung; Kondenswasser-Prüfklimate.Deutsches Institut für Normung e.V. Berlin.

DIN 50018-Ausgabe:1997-06 (1997) Prüfung im Kondenswasser-Wechselklima mit schwefeldioxidhaltiger Atmosphäre. Deutsches Institut für Normung e.V. Berlin.

Donia G., (2000) Inspector 2000 project. Ceramic World Review, 10, 37: 216-219

Elsen, J. (1996) Diagnostic des pierres naturelles et optimisation de leurs techniques de mise en œuvre, T.2 : Le comportement des granits sous l'influence de l'exposition en atmosphère acide. Centre scientifique et technique de la construction (Ed.)., Bruxelles.

Elsen, J. (1998) Durability of Granites for Construction. Aardk. Mededel., 9: 35-40.

Gonzalez, C; and Woods, R. (1992) Digital image processing. Addision Wesley (ed)

Holst, G. C. (1998) CCD Arrays, Cameras and Displays, SPIE Optical Engineering Press, Washington, p. 127-131.

Lebrun, V. Bonino, E. Nivart, J.-F., Pirard, E. (1999) Development of specific acquisition techniques for field imaging-Applications to outcrops and marbles. Geovision, Int. Symp. on imaging applications in geology, pp 165-168.

MacAdam, D. L. (1942) Visual sensitivities to color differences in daylight. J. Opt. Soc. Am, 32: 247-273.

Maccari, A., (1998) ASPECT: an intelligent sorting system. Ceramic World Review, 8, 28: 138-141

Marszalec, E. and Pietikäinen M. (1996) Some aspect of RGB vision and its applications in industry. International Journal of Pattern Recognition and Artificial Intelligence. 10, 1: 55-72.

Marszalec, E. and Pietikäinen M. (1997) Color measurements based on a color camera. In Rolp-Jürgen Ahlers, Philippe Réfrégier (eds) New image processing techniques and applications: algorithms, methods and components II., pp170-181, Proc. SPIE Vol. 3101, June 1997.

Muge, F. et al. (1997) Caracterization of ornamental stones standards by image analysis of slab surface (COSS) Eurominerals'97, II Int. Cong. of Natural and Industrial stones, Lisboa

Munsell, A. H. (1975) A Color Notation : an illustrated system defining all colors and their relations by measured scales of hue, value and chroma. Munsell Color Cy, Baltimore.

Pirard, E. Lebrun, V. Nivart, J.-F. (1999) Optimal acquisition of video images in reflected light microscopy. Microscopy and Analysis, 60: 9-11

Russ, J. C. (1999) The Image Processing Handbook. 3rd ed. CRC press (ed), Boca Raton, 771 p.

Soille, P. (2000) Morphological Image Analysis. Springer (ed), Berlin, 316 p.